Journal of Sound and Vibration (1999) **228**(1), 37–50
Article No. jsvi.1999.2401, available online at http://www.idealibrary.com on IDEAL®

TRANSIENT RESPONSE OF ROTATING LAMINATED PLATES WITH INTERFACIAL FRICTION UNDER ACCELERATING CONDITIONS

J. S. RAO

Department of Mechanical Engineering, Indian Institute of Technology, New Delhi 110016, *India*

AND

Y. D. YU and T. N. SHIAU

Graduate Institute of Mechanical Engineering, National Chung Cheng University, Chia-Yi, Taiwan, Republic of China

(*Received* 28 *April* 1997, *and in final form* 19 *May* 1999)

This paper is concerned with laminated plates mounted on a rotating disk under accelerating conditions. Interfacial friction is included at specified locations on the plate. The effects of in-plane loads and non-linear Coriolis forces are included. An eight noded isoparametric element is derived for the analysis. Under the action of combined accelerating conditions and Coriolis forces, it is shown that the blade is subjected to shock forces. Employing the Newmark direct integration method, the results obtained are presented.

1. INTRODUCTION

Gas turbine and compressor blades are most flexible elements and susceptible to fatigue failures. They are subjected to nozzle passing excitation and go through several critical speeds before reaching the operating speed. To limit the resonant response at these criticals under transient conditions, a good damping design is practised through interfacial slipping surfaces. The blades themselves can be treated as beams or plates depending on the blade aspect ratio and laminated plates offer light weight and high strength for the blading.

The application of plate theory to blade vibration problems has been considered by several authors which include Petricone and Sisto [1], Dokainish and Rawtani [2], MacBain [3], Gupta and Rao [4] amongst others. The steady state response and stability of rotating laminated plates is studied by Shiau *et al.* [5].

Damping studies form an important aspect of blade vibration studies, since it plays an important role in limiting the resonant vibrations. These models can be broadly divided into two major categories: (1) macro slip models, e.g., Sinha and Griffin [6] and (2) micro slip models, e.g., Menq *et al.* [7]. A non-linear damping

0022-460X/99/460037 + 14 $30.00/0

model was proposed by Rao *et al.* [8] based on experiments and was utilized in determining response of blades under transient conditions but without taking into account the Coriolis forces [9]. There are finite element packages which have friction elements and transient analysis capabilities, e.g., ANSYS [10] but which cannot handle the effect of Coriolis accelerations.

The equations of motion of beam-type blades taking into account of accelerating conditions as well as Coriolis forces were derived by Vyas and Rao [11], which were later solved by them in reference [12]. A significant aspect of this work is the development of shock forces which increase the response under high accelerating conditions. Here, the work of Shiau *et al.* [5] of rotating laminated plates is extended to account for the Coriolis forces in the presence of accelerating conditions and under the influence of interfacial friction.

2. EQUATIONS OF MOTION

We first set up the kinetic energy expression of a rotating laminated plate shown in Figure 1.

2.1. KINETIC ENERGY

The position vector of a typical point P on the blade after deformation can be expressed as

$$\mathbf{OP}' = \begin{Bmatrix} x \\ y \\ z \end{Bmatrix} + \begin{Bmatrix} u \\ v \\ w \end{Bmatrix}$$

$$\{\bar{x}\} + \{d\}. \tag{1}$$

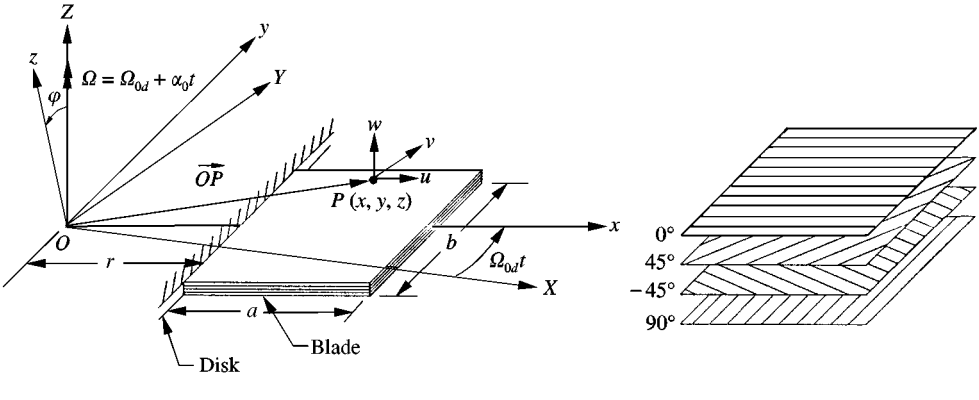

Figure 1. Configuration of the composite laminate blade.

Let the blade rotate under constant angular acceleration $\mathbf{a} = \{a_x \quad a_y \quad a_z\}^{\mathrm{T}}$ starting with an initial angular velocity $\mathbf{\Omega}_0 = \{\Omega_{0x} \quad \Omega_{0y} \quad \Omega_{0z}\}^{\mathrm{T}}$ where

$$a_x = 0, \quad \Omega_{0x} = 0,$$

$$a_y = a_0 \sin\varphi, \quad \Omega_{0y} = \Omega_{0d} \sin\varphi,$$

$$a_z = a_0 \cos\varphi, \quad \Omega_{0z} = \Omega_{0d} \cos\varphi.$$

The angular velocity at any instant t is

$$\mathbf{\Omega} = \begin{Bmatrix} \Omega_x \\ \Omega_y \\ \Omega_z \end{Bmatrix} = \begin{Bmatrix} \Omega_{0x} \\ \Omega_{0y} \\ \Omega_{0z} \end{Bmatrix} + \begin{Bmatrix} a_x \\ a_y \\ a_z \end{Bmatrix} t.$$

Then, the velocity of point P is

$$\mathbf{v} = \mathbf{OP}' + \mathbf{\Omega} \times \mathbf{OP}' = \begin{Bmatrix} \dot{u} \\ \dot{v} \\ \dot{w} \end{Bmatrix} + \begin{Bmatrix} 0 & -\Omega_z & \Omega_y \\ \Omega_z & 0 & -\Omega_x \\ -\Omega_y & \Omega_x & 0 \end{Bmatrix} + \begin{Bmatrix} x+u \\ y+v \\ z+w \end{Bmatrix}$$

$$= \{\dot{d}\} + [A](\{\bar{x}\} + \{d\}). \tag{2}$$

The kinetic energy of the composite plate is then given by

$$T = \frac{1}{2} \iiint_V \rho \mathbf{v} \cdot \mathbf{v} \, \mathrm{d}V$$

$$= T_2 + T_1 + T_0, \tag{3}$$

where

$$T_2 = \frac{1}{2} \iiint_V \rho \{\dot{d}\}^{\mathrm{T}} \{\dot{d}\} \, \mathrm{d}V,$$

$$T_1 = \iiint_V \rho \{\dot{d}\}^{\mathrm{T}} [A] \{d\} \, \mathrm{d}V + \iiint_V \rho \{\dot{d}\}^{\mathrm{T}} [A] \{\bar{x}\} \, \mathrm{d}V,$$

$$T_0 = \frac{1}{2} \iiint_V \rho \{d\}^{\mathrm{T}} [A]^{\mathrm{T}} [A] \{d\} \, \mathrm{d}V + \frac{1}{2} \iiint_V \rho \{\bar{x}\}^{\mathrm{T}} [A]^{\mathrm{T}} [A] \{x\} \, \mathrm{d}V$$

$$+ \iiint_V \rho \{d\}^{\mathrm{T}} [A]^{\mathrm{T}} [A] \{\bar{x}\} \, \mathrm{d}V \tag{4}$$

2.2. POTENTIAL ENERGY

The total potential energy of the plate can be shown to be

$$U = U_b + U_p, \tag{5}$$

where

$$U_b = \frac{1}{2}\iiint_V \{\sigma_x \quad \sigma_y \quad \sigma_{xy} \quad \sigma_{yz} \quad \sigma_{zx}\} \begin{Bmatrix} \varepsilon_x \\ \varepsilon_y \\ \varepsilon_{xy} \\ \varepsilon_{yz} \\ \varepsilon_{zx} \end{Bmatrix} \mathrm{d}V$$

$$= \frac{1}{2}\iiint_V \{\sigma\}^{\mathrm{T}}\{\varepsilon\}\,\mathrm{d}V, \tag{6}$$

$$U_p = \iiint_V \{\sigma_x^0 \quad \sigma_y^0 \quad \sigma_{xy}^0\} \begin{Bmatrix} \frac{1}{2}w_{,x}^2 \\ \frac{1}{2}w_{,y}^2 \\ w_{,x}\, w_{,y} \end{Bmatrix} \mathrm{d}V$$

$$= \frac{1}{2}\iiint_V \{w_{,x} \quad w_{,y}\} \begin{bmatrix} \sigma_x^0 & \sigma_{xy}^0 \\ \sigma_{xy}^0 & \sigma_y^0 \end{bmatrix} \begin{Bmatrix} w_{,x} \\ w_{,y} \end{Bmatrix} \mathrm{d}V$$

$$= \frac{1}{2}\iiint_V \{\varepsilon_g\}^{\mathrm{T}}[\sigma^0]\{\varepsilon_g\}\,\mathrm{d}V, \tag{7}$$

where $[\sigma^0]$ are initial stresses of the blade due to the effect of the centrifugal force of the rotating plate. For the laminated plate, the stress–strain relationship is

$$\{\sigma\} = [\bar{Q}]\,\{\varepsilon\}, \tag{8}$$

where $[\bar{Q}]$ is the reduced stiffness matrix [13] and the strain energy due to bending is

$$U_b = \frac{1}{2}\iiint_V \{\varepsilon\}^{\mathrm{T}}[\bar{Q}]\{\varepsilon\}\,\mathrm{d}V. \tag{9}$$

2.3. FINITE ELEMENT

An eight-noded isoparametric element is adopted. The co-ordinate systems and configuration of the element can be taken from Yang [14]:

$$x = \sum_{i=l}^{8} \phi_i x_i, \quad y = \sum_{i=1}^{8} \phi_i y_i, \quad z = \sum_{i=1}^{8} \phi_i z_i,$$

which in matrix from is

$$\{\bar{x}\} = [N_1]\,\{\underline{x}_n^{(l)}\}, \tag{10}$$

where matrix $[N_1]$ can be taken from Shiau *et al.* [5] and

$$\{\underline{x}_n^{(l)}\} = \{x_1 \quad y_1 \quad z_1 \ldots y_8 \quad z_8\}.$$

Mindlin's plate theory is adopted and the displacement components are expressed as

$$u = u_0(x, y, t) + z\psi_x(x, y, t) = \sum_{i=1}^{8} \phi_i u_i + z \sum_{i=1}^{8} \phi_i \psi_{xi},$$
$$v = v_0(x, y, t) + z\psi_y(x, y, t) = \sum_{i=1}^{8} \phi_i v_i + z \sum_{i=1}^{8} \phi_i \psi_{yi},$$
$$w = w_0(x, y, t) = \sum_{i=1}^{8} \phi_i w_i, \tag{11}$$

which in matrix form are

$$\{d\} = [N_2]\{q\}, \tag{12}$$

where $[N_2]$ can be taken from Shiau *et al.* [5] and $\{q\} = \{u_1 \ v_1 \ w_1 \ \psi_{x1} \ \psi_{y1} \dots\}^{\mathrm{T}}$ is the nodal displacement vector. Now, the strain displacement relations are written as

$$\{\varepsilon\} = [N_3]\{q\},$$
$$\{\varepsilon_g\} = [N_4]\{q\}, \tag{13}$$

where $[N_3]$, $[N_4]$ can be taken from Shiau *et al.* [5]. Making use of the Jacobian matrix to get the partial derivatives with respect to local co-ordinates and the Lagrangian approach, the equations of motion for the element can be obtained as

$$[\hat{M}]\{\ddot{q}\} + [\hat{G}]\{\dot{q}\} + [\hat{K}]\{q\} + \{\hat{f}_a\} + \{\hat{f}_c\} = \{\hat{F}_g\}, \tag{14}$$

where

$$[\hat{M}] = \iiint \rho [N_2]^{\mathrm{T}} [N_2] \, \mathrm{d}V,$$
$$[\hat{G}] = 2 \iiint \rho [N_2]^{\mathrm{T}} [A] [N_2] \, \mathrm{d}V,$$
$$[\hat{K}] = -\iiint \rho [N_2]^{\mathrm{T}} [A]^{\mathrm{T}} [A] [N_2] \, \mathrm{d}V + \iiint [N_3]^{\mathrm{T}} [\bar{Q}] [N_3] \, \mathrm{d}V + \iiint \rho [N_2]^{\mathrm{T}} [A] [N_2] \, \mathrm{d}V$$
$$= [\hat{K}_r] + [\hat{K}_e] + [\hat{K}_a],$$
$$\{\hat{f}_a\} = -\iiint \rho [N_2]^{\mathrm{T}} [A]^{\mathrm{T}} [N_1] \, \mathrm{d}V \{\underline{x}_n^{(l)}\},$$
$$\{\hat{f}_c\} = -\iiint \rho [N_2]^{\mathrm{T}} [A]^{\mathrm{T}} [A] [N_1] \, \mathrm{d}V \{\underline{x}_n^{(l)}\}.$$

The initial displacement vector $\{q_c\}$ due to centrifugal force field is obtained from $[\hat{K}_e]\{q_c\} = \{\hat{f}_c\}$ and the corresponding initial stress vector for pre-vibration

condition is determined from $\{\sigma^0\} = [\bar{Q}][N_2]\{q_c\}$. Then, with the help of the in-plane potential energy in equation (7) and Lagrangian approach, the geometric stiffness matrix is obtained as

$$[\hat{K}_g] = \iiint \rho [N_4]^{\mathrm{T}} \{\sigma^0\} [N_4] \, \mathrm{d}V. \tag{15}$$

Equation (14) now becomes

$$[\hat{M}]\{\ddot{q}\} + [\hat{G}]\{\dot{q}\} + ([\hat{K}] + [\hat{K}_g])\{q\} + \{\hat{f}_a\} = \{\hat{F}_g\}. \tag{16}$$

After assembling the elemental equations, we get

$$[M]\{\ddot{\delta}\} + [G]\{\dot{\delta}\} + [K]\{\delta\} = -\{f_a\} + \{F_g\}. \tag{17}$$

The generalized force vector $\{F_g\} = \{F_{NPF}\} + \{F_{ndf}\}$ in the above equation consists of nozzle passing harmonic force and the non-linear dry friction force. The nozzle passing force is

$$\mathbf{F}_{NPF} = \begin{Bmatrix} F_1 \\ F_2 \\ F_3 \end{Bmatrix} \cos(\Omega_p t - \Phi_p). \tag{18}$$

The elemental force vector is

$$\{\mathbf{F}_{NPF}\} = \left(\iint_A [N_2] \begin{Bmatrix} F_1 \\ F_2 \\ F_3 \end{Bmatrix} \mathrm{d}A \right) \cos(\Omega_p t - \Phi_p). \tag{19}$$

The non-linear dry friction force is accounted by assuming that there is macro slip (see Figures 2 and 3). The component f^i_{ndf} at the ith node of the vector $\{F_{ndf}\}$ is expressed as

$$f^i_{ndf} = \left\{ \begin{matrix} K_G(\delta_i - z_i) & \text{when } K_G|\delta_i - z_i| \leqslant \mu R \\ \mu R \operatorname{sign}(\dot{z}_i) & \text{when } K_G|\delta_i - z_i| \geqslant \mu R \end{matrix} \right\} \text{shroud location}$$
$$= 0 \quad \text{otherwise.} \tag{20}$$

3. NUMERICAL EXAMPLE

The solution of equations (17) is obtained by using the Newmark method. A $[0/\pm 45/90]_{\mathrm{sym}}$ composite mid-plane symmetric laminate blade with $a =$ 0·1524 m, $b =$ 0·0381 m, $t =$ 0·000528 m mounted on a 0·381 m radius disk is considered. The blade aspect ratio is 4. The material properties of graphite are: Young's modulii 128 and 11 GPa, shear modulii 4·48, 4·48 and 1·53 GPa, the Poisson ratio 0·25, thickness 0·00013 m and the density 1500 kg/m^3. The stiffness of the friction damper in the direction of relative motion is taken as 3500 N/m. The blade is discretized into four elements as shown in Figure 4.

The response of the blade tip center with zero initial speed and constant angular acceleration 16 000 r.p.m./min, setting angle 90°, with a non-linear dry friction force

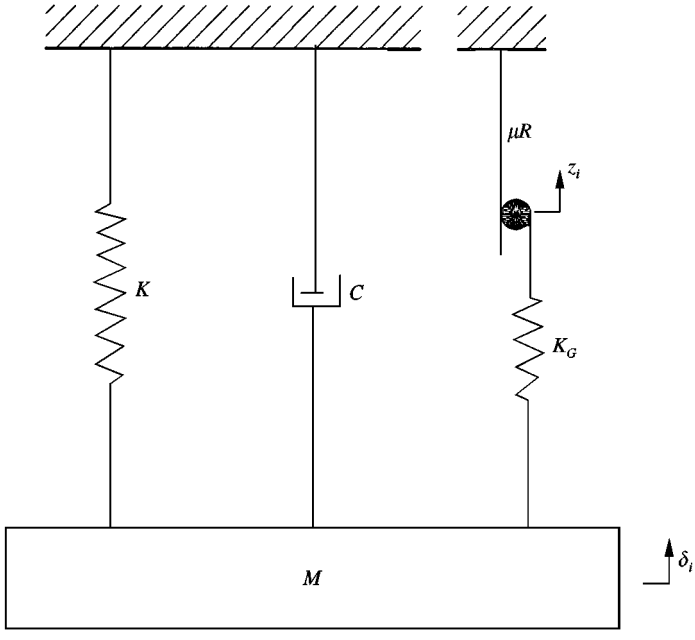

Figure 2. Model of frictional damping system.

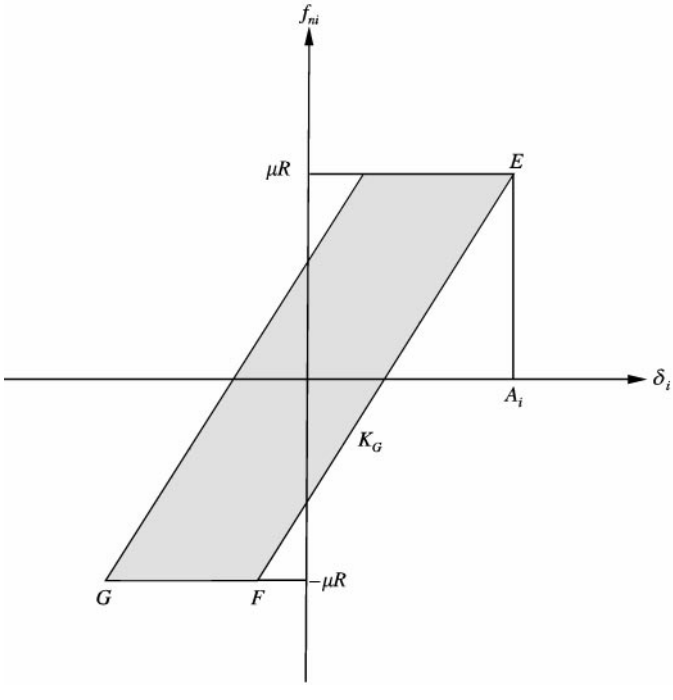

Figure 3. Loop friction force versus response.

$\mu R/f_0 = 0{\cdot}02$ applied at node 19 is shown in Figure 5. The frequency of the response is 230 cps corresponding to the first natural frequency of the blade. Because of acceleration, the blade experiences a sudden shock and the resulting peak-to-peak

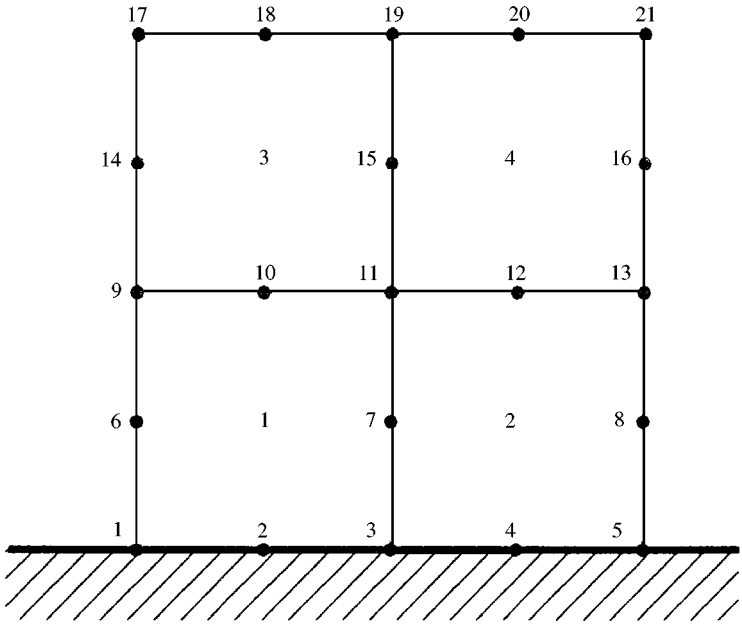

Figure 4. Four element mesh of the blade.

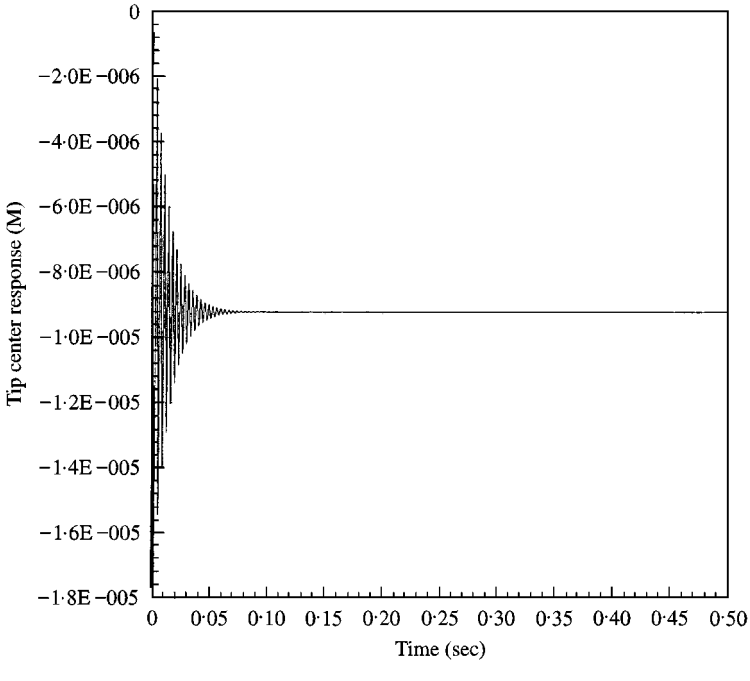

Figure 5. Response at $a_0 = 16\,000$ r.p.m./min, $\Omega_{0d} = 0$, $\varphi = 90^\circ$ and $\mu R/f_0 = 0{\cdot}02$.

vibration of 18 μm decays in the presence of the friction damping. The pseudo-static response is about 9 μm. When the acceleration is decreased to 3200 r.p.m./min, the response also decreases to nearly 3·5 μm peak to peak settling down to a pseudo-static response of 1·8 μm as shown in Figure 6.

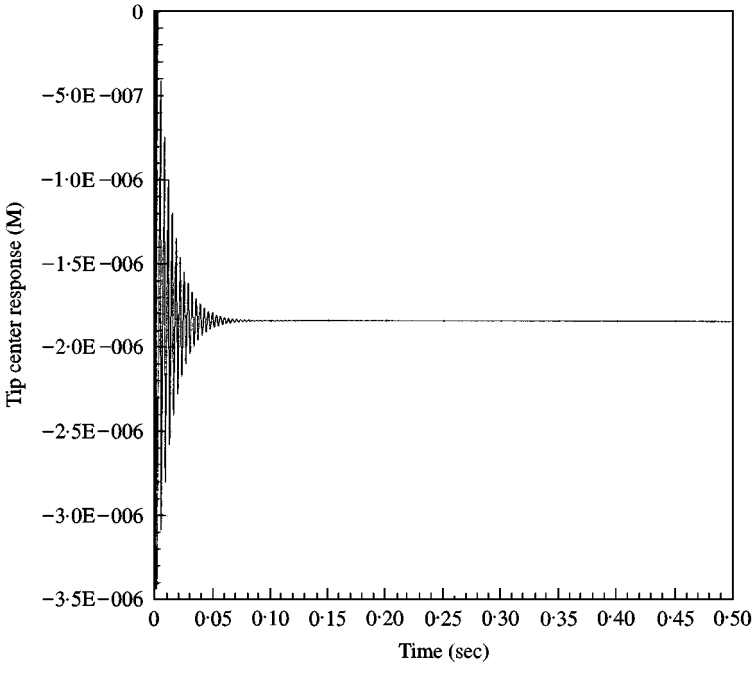

Figure 6. Response at $a_0 = 3200$ r.p.m./min, $\Omega_{0d} = 0$, $\varphi = 90^\circ$ and $\mu R/f_0 = 0{\cdot}02$.

We can consider here a simple case of a spring–mass system with a natural frequency $\omega_0 = 230$ cps (1445·13 rad/s) subjected to a sudden base acceleration $a_0 = 16\,000$ r.p.m/min (27·925 rad/s/s). The peak-to-peak response of the mass is then $2a_0/\omega_0^2 = 26{\cdot}74$ μm. In the rotating plate example with a non-linear dry friction force above the peak-to-peak response is 18 μm, a value that is comparable to the undamped single-degree-of-freedom system. At 3200 r.p.m./min acceleration, the peak-to-peak response of the single-degree-of-freedom system is a fifth of 26·74 μm = 5·348 μm. For the plate example, the response at 3200 r.p.m./min is 3·5 μm which is 5·1 times less than the response at 16 000 r.p.m./min.

Next, a nozzle passing harmonic distributed force is applied over the entire blade with a transverse force $= 10\cos\Omega_p t$ N/m^2 and chordwise force $= 10\cos\Omega_p t$ N/m^2. Figure 7 shows the transient and forced vibration response for $\Omega_{0d}/\omega_{n1} = 0{\cdot}5$, $\Omega_p/\omega_{n1} = 1{\cdot}0$ and $a_0 = 16\,000$ r.p.m/min. To begin with, the blade is assumed to run at a constant speed, and is accelerated at 0·2 s for a period of 0·5 s. As soon as the blade begins to rotate, a transient is developed which decays in the presence of friction and settles to a steady state forced vibration amplitude of 2·2 μm in about 0·1 s. When the blade is accelerated at 0·2 s it experiences a shock and the mean equilibrium shifts to a new level with a substantially large dynamic displacement. The transient vibration dies out in about 0·1 s again and settles to the steady state value. However, there is a residual mean deflection of nearly 7 μm.

In Figure 8, the response of the blade for a lower value of acceleration $a_0 = 3200$ r.p.m/min is given. One can see a similar behavior as in Figure 7. The pseudo-static deflection, however, is about 1·4 μm only.

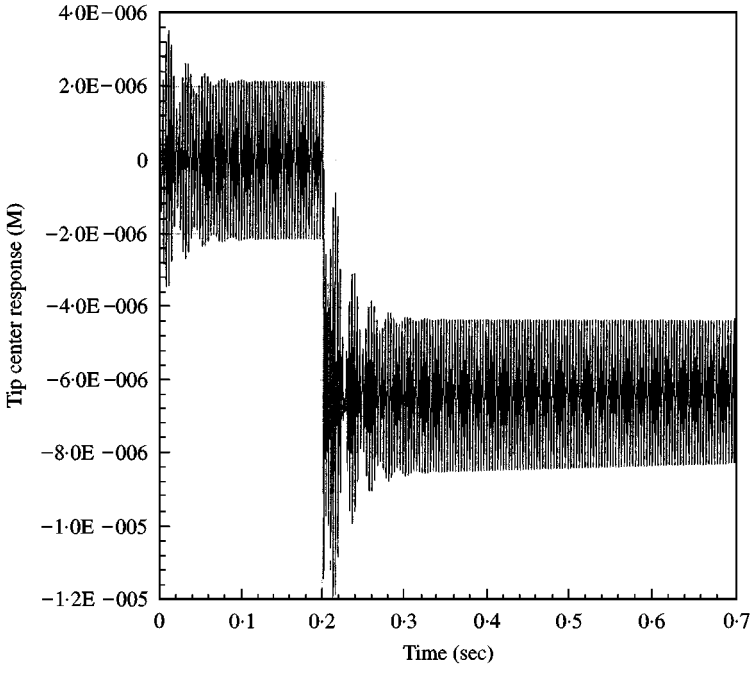

Figure 7. Response at $a_0 = 16\,000$ r.p.m./min, $\Omega_{0d}/\omega_{n1} = 0{\cdot}5$, $\varphi = 90^\circ$, $\Omega_p/\omega_{n1} = 1{\cdot}0$ and $\mu R/f_0 = 0{\cdot}02$.

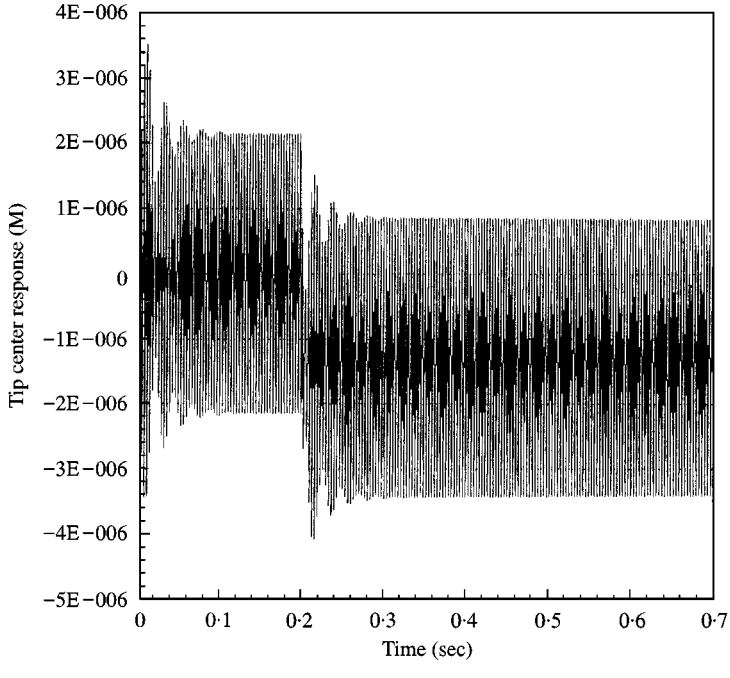

Figure 8. Response at $a_0 = 3200$ r.p.m./min, $\Omega_{0d}/\omega_{n1} = 0{\cdot}5$, $\varphi = 90^\circ$, $\Omega_p/\omega_{n1} = 1{\cdot}0$ and $\mu R/f_0 = 0{\cdot}02$.

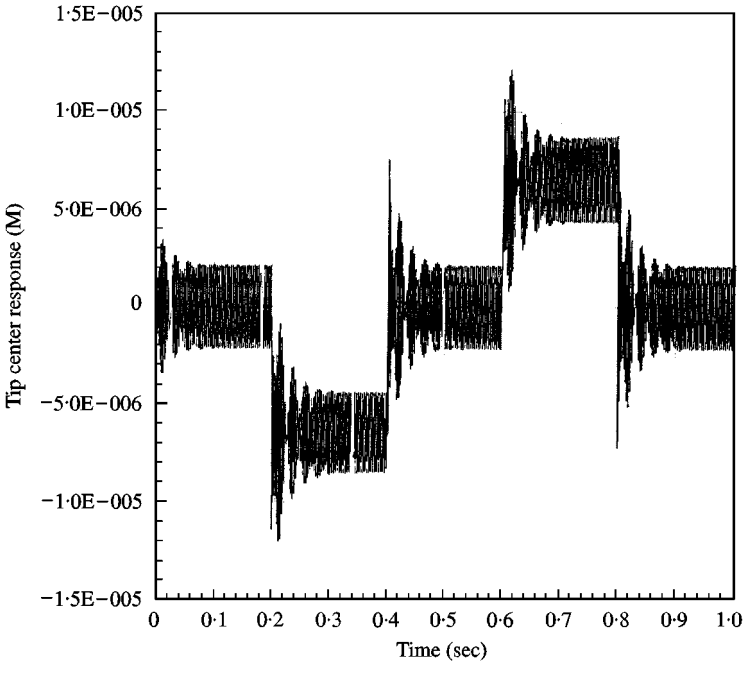

Figure 9. Response at $a_0 = \pm 16\,000$ r.p.m./min, $\Omega_{0d}/\omega_{n1} = 0{\cdot}5$, $\varphi = 90^\circ$, $\Omega_p/\omega_{n1} = 1{\cdot}0$ and $\mu R/f_0 = 0{\cdot}02$.

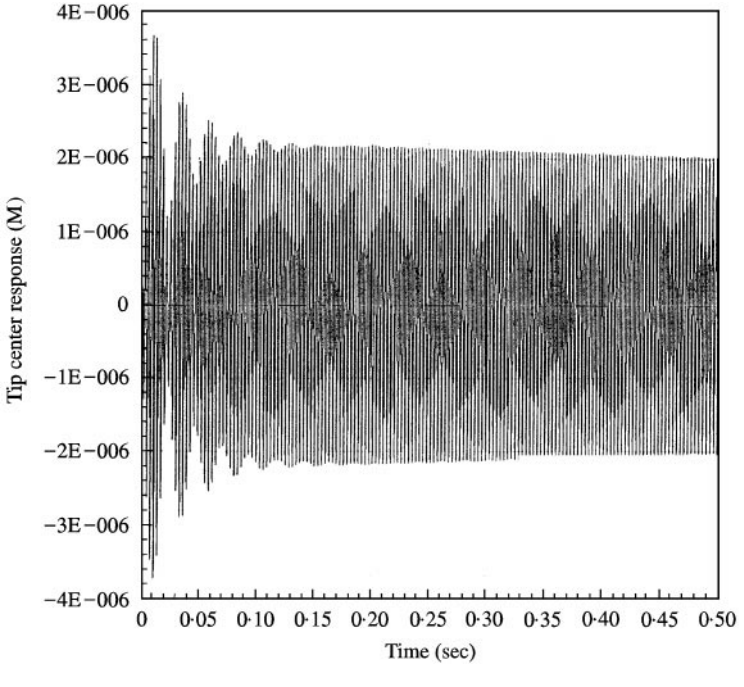

Figure 10. Response at $a_0 = 16\,000$ r.p.m./min, $\Omega_{0d}/\omega_{n1} = 0{\cdot}5$, $\varphi = 0^\circ$, $\Omega_p/\omega_{n1} = 1{\cdot}0$ and $\mu R/f_0 = 0{\cdot}02$.

Next the effect of accelerating and decelerating the blade is shown in Figure 9 by $a_0 = \pm 16\,000$ r.p.m./min. After an initial constant running speed operation for 0·2 s, the blade is accelerated; then at 0·4 s the acceleration is cut off. It is then decelerated, at 0·6 s, and the deceleration is cut off at 0·8 s. Each time the blade is subjected to an acceleration, there is a change in the pseudo-static deflection and that the transient dies out in less than 0·1 s.

Figure 10 shows the response with the blade setting angle equal to zero, first with $a_0 = 0$ for 0·2 s and then with $a_0 = 16\,000$ r.p.m./min for 0·3 s. We find that there is practically no pseudo-static response, since the second moment of area is very large in the fixed frame Z-axis direction as shown in Figure 1.

4. CONCLUSIONS

A finite element analysis for rotating laminated plates under accelerating and decelerating conditions including Coriolis forces is proposed. The equations of motion are solved by the direct integration method. It is shown that the blades are subjected to a shock force and that pseudo-static deflections larger than the dynamic response can occur while crossing resonance.

REFERENCES

1. R. Petricone and F. Sisto 1970 *ASME 70-GT-94*. Vibration characteristics of low aspect ratio compressor blades.
2. M. A. Dokainish and S. Rawtani 1973 *International Journal of Numerical Methods in Engineering* **3**, 233. Vibration analysis of rotating cantilever plates.
3. J. C. Macbain 1975 *Journal of Aircraft* **12**, 343. Vibratory behaviour of twisted cantilever plates.
4. K. Gupta and J. S. Rao 1978 *Journal of Mechanical Design ASME* **100**, 528. Torsional vibration of pre-twisted cantilever plates.
5. T. N. Shiau, J. S. Rao, Y. D. Yu and S. T. Choi 1998 *Journal of Engineering for Gas Turbines and Power, Transactions of ASME* **120**, 131. Steady state response and stability of rotating composite blades with frictional damping.
6. A. Sinha and J. H. Griffin 1984 *Journal of Engineering for Gas Turbines and Power, ASME* **106**, 65. Effects of static friction on the forced response of frictionally damped turbine blades.
7. C. M. Menq, J. H. Griffin and J. Bialek 1986 *Journal of Sound and Vibration* **107**, 279. The influence of microslip on vibration response.
8. J. S. Rao, K. Gupta and N. S. Vyas 1986 *Shock and Vibration Bulletin* **56**, Pt. 2, 109. Blade damping measurement in a spin rig with nozzle passing excitation simulated by electromagnets.
9. J. S. Rao and N. S. Vyas 1996 *Journal of Engineering for Gas Turbines and Power, Transactions of ASME* **118**, 424. Determination of blade stresses under constant speed and transient conditions with nonlinear damping.
10. *ANSYS Engineering Analysis System*. Houston, PA 15342, USA: Swanson Analysis Systems Inc.
11. N. S. Vyas and J. S. Rao 1992 *Journal of Sound and Vibration* **155**, 327. Equations of motion of a blade rotating with variable angular velocity.
12. N. S. Vyas and J. S. Rao 1994 *Journal of Sound and Vibration* **176**, 531. Shock in rotor blades during speed changes.

13. J. E. ASHTON and J. M. WHITNEY 1970 *Theory of Laminated Plates*. Technomic.
14. T. Y. YANG 1986 *Finite Element Structural Analysis*. Englewood Cliffs, NJ: Prentice Hall.

APPENDIX: NOMENCLATURE

$[A]$	angular velocity matrix
$\{d\}$	displacement vector
F_1, F_2, F_3	nozzle passing force components
$\mathbf{F}_{NPF}$	nozzle passing force vector
$\{F_g\}$	external force vector
$\{f_a\}$	pseudo-static tangential force vector
$\{f_c\}$	centrifugal force vector
f_{ndf}	non-linear dry friction force
$[G]$	gyroscopic matrix
K_G	damper stiffness
$[K]$	stiffness matrix
$[K_a]$	acceleration stiffness matrix
$[K_e]$	elastic stiffness matrix
$[K_g]$	rotary stiffness matrix
$[K_r]$	geometric stiffness matrix
$[M]$	mass matrix
$[N_i]$	shape function and related matrices, see Shiau *et al.* [5]
$[\bar{Q}]$	reduced stiffness matrix
$\{q\}$	nodal displacement vector
$\{q_c\}$	initial displacement vector
R	normal preload
t	time
T	kinetic energy
U	potential energy
u, v, w	displacements
$\mathbf{v}$	velocity vector
$\{\bar{x}\}$	co-ordinates vector
$\underline{x}_n^{(l)}$	nodal co-ordinates vector
x, y, z	rotating co-ordinates
z_i	displacement of friction damper
$\mathbf{a}$	angular acceleration vector
a_x, a_y, a_z	acceleration components
$\{\delta\}$	global displacement vector
$\varepsilon_x \cdots$	strain components
$\{\varepsilon\}$	strain vector
$\{\varepsilon_g\}$	gradient vector
μ	coefficient of friction
ϱ	density
$\sigma_x \cdots$	stress components
$\{\sigma\}$	stress vector
$[\sigma^0]$	initial stresses
ϕ	shape functions, see reference [14]
φ	setting angle
ψ_x, ψ_y	slopes
$\mathbf{\Omega}_0$	initial angular velocity
Ω_p	nozzle passing excitation frequency

Ω_{0d} angular velocity of disk
$\Omega_{0x} \cdots$ angular velocity components
$\dot{}$ denotes differentiation with time
$,^{x}$ denotes differentiation with respect to x...
$\frown$ denotes elemental matrices